

³¹P CP/MAS NMR of polycrystalline and immobilized phosphines and catalysts with fast sample spinning

S. Reinhard and J. Blümel*

Organisch-Chemisches Institut, Universität Heidelberg, Im Neuenheimer Feld 270, 69120 Heidelberg, Germany

Received 23 October 2002; Revised 22 January 2003; Accepted 23 January 2003

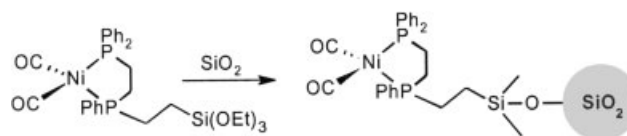
Cross-polarization (CP) at fast magic angle spinning (MAS) frequencies leads to a splitting of the Hartmann–Hahn (HH) matching profile into a centerband and additional bands of higher orders. The matching profiles differ with the substance categories. Therefore, signal intensity is usually lost, when e.g. the routine standard $\text{NH}_4\text{H}_2\text{PO}_4$ is used for optimizing the ^1H – ^{31}P HH match prior to measuring phosphines and their metal complexes in polycrystalline or immobilized form. Here, a variety of model compounds, such as $\text{Ph}_2\text{PCH}_2\text{CH}_2\text{PPh}_2$ and $(\text{CO})_2\text{Ni}(\text{PPh}_3)_2$, which can be used as ^{31}P CP standards for analogous substances or materials are presented. Investigating the influences of MAS frequency, contact time, ^1H pulse power and sample volume on the matching profiles of the model compounds leads to general trends. Thereby, a new strategy for measuring difficult samples with CP at high MAS rates has been developed: their optimum CP parameters are derived from the most intense maxima in the HH matching profiles of the corresponding model compounds. This new strategy is compared with variations of a conventional ramp sequence. Although the latter generally provide smaller signal half-widths, the new strategy leads to higher signal intensities. The new method was successfully applied to polycrystalline and immobilized phosphines and catalysts. Copyright © 2003 John Wiley & Sons, Ltd.

KEYWORDS: NMR; ^{31}P NMR; CP/MAS; fast spinning; HH matching profiles; immobilized catalysts; immobilized phosphines; silica supports; rhodium and nickel catalysts

INTRODUCTION

There has been enormous interest recently in species tethered to solid supports, ranging from combinatorial chemistry¹ through solid-phase synthesis² and new stationary materials for reversed-phase chromatography^{3,4} to catalysts immobilized on solid supports.^{5–8}

For the last decade, we have been investigating various surface-bound catalysts, a subject of commercial and academic interest. Among many advantages, they incorporate the most favorable characteristics of well designable homogeneous catalysts, such as high selectivity and activity. At the same time, they display the best properties of heterogeneous catalysts, such as easy separation from the reaction mixture and recycling.^{8–13} In the case of immobilized carbonylnickel and Wilkinson-type catalysts bound to silica via bifunctional monodentate and chelating phosphine ligands, such as that displayed in Scheme 1, the basic expectations have been fulfilled: the immobilized catalysts are highly active with respect to the cyclotrimerization of acetylenes^{10,11} and hydrogenation of olefins,^{8,12} and can easily be recycled many times.^{8,10–12}



Scheme 1. Example of a carbonylnickel complex being immobilized on silica via a chelating phosphine linker.

In order to develop this chemistry to its full potential, we first had to investigate in detail the reactions of the linker group $\text{Si}(\text{OEt})_3$ with the silica surface,^{14–18} because the manner of its binding is crucial for the later performance of the catalyst: if the reaction conditions are too harsh during the immobilization step, side reactions of the phosphines with the silica surface occur, which are detrimental for later catalysis.¹⁷ If the number of residual ethoxy groups is not determined properly, miscalculations of surface coverages,^{14–16} and thereby misjudgements about the performance of the catalyst, result. Finally, if the linkers are not bound strongly in a covalent manner, but are just physically adsorbed, subsequent leaching of the catalyst will be inevitable.^{14,18} Leaching can also occur if the metal moieties are not bound strongly enough by the linkers, as could be demonstrated in the case of carbonylnickel catalysts.¹¹ This can be prevented by using chelating phosphine ligands such as those described in Refs 8 and 19.

*Correspondence to: J. Blümel, Organisch-Chemisches Institut, Universität Heidelberg, Im Neuenheimer Feld 270, 69120 Heidelberg, Germany. E-mail: J.Bluelmel@urz.uni-heidelberg.de
Contract/grant sponsor: Deutsche Forschungsgemeinschaft.
Contract/grant sponsor: Fonds der Chemischen Industrie.

As an analytical tool for surface-supported species, suspension NMR can deliver incisive results.^{18–21} The purity of a large number of routine samples can be checked easily and quickly. Species that are merely physically in contrast to covalently bound are obvious in suspension NMR spectra, and leaching can be detected directly.¹⁸ Furthermore, from the linewidths of the suspension NMR signals the mobilities of surface-bound species can be estimated.^{18,20} However, owing to the resulting broad signals, suspension NMR has its limitations, if the chemical shift anisotropies (CSA)²² of the investigated metal complexes are large.²⁰ In this event, the classical and most powerful analytical method for studying these amorphous materials is solid-state NMR.^{8–19,23–29}

The trend in solid-state NMR for species with large chemical shift anisotropies is towards increased magic angle spinning (MAS) frequencies in order to enhance the signal intensity of the isotropic line while reducing the number of rotational sidebands. This also minimizes the problem of signals overlapping with spinning sidebands. For special purposes such as ¹H MAS NMR, rotational frequencies of up to 50 kHz can be applied. In the case of multinuclear measurements, however, routine spinning speeds of about 15 kHz are used today with still rather robust 4 mm diameter ZrO₂ or Si₃N₄ rotors. Compared with the former 7 mm rotors, the reduced sample size is favorable, as less substance is needed to fill the rotor. On the other hand, the reduced amount of sample is a disadvantage for very dilute species, such as molecules bound merely to the surface of some bulk material. For example, a typical value of the phosphorus content of our immobilized catalysts would be about 1 wt%.

In order to enhance the multinuclear signal intensities, cross polarization (CP),^{23–28,30–34} involving the transfer of magnetization from abundant nuclei, usually from protons, to the dilute nuclei (e.g. ³¹P, ¹³C, ²⁹Si), which also reduces the recycle delays, can be used. Indeed, CP works well with spinning speeds of up to 4 kHz, as for example our previous work shows.^{8–17} The Hartmann–Hahn (HH) matching condition for CP, $\omega(^1\text{H}) = \gamma(^1\text{H})B_1(^1\text{H}) = \gamma(^{31}\text{P})B_1(^{31}\text{P}) = \omega(^{31}\text{P})$, was optimized for ³¹P NMR using the standard polycrystalline NH₄H₂PO₄ (1), and then these same values could successfully be applied to real samples that did not show a visible FID with only a few transients. However, owing to the larger CSA, metal complexes in general,²² and our rhodium and nickel catalysts in particular,^{8,10} display a multitude of spinning sidebands in spectra measured at only 4–8 kHz. Therefore, a faster spinning is a prerequisite for attaining a signal especially of merely surface-bound catalysts. At this point a major problem arises: as already known for some time, with faster spinning the HH matching profile splits into a center band with sidebands of first, second and higher orders about the spinning frequency apart from each other. This phenomenon has been very well described^{32,35–37} and has also been studied more theoretically.^{38–42} Whereas for molecular substances, accidentally not hitting the optimum HH match precisely any longer only leads to a loss of signal intensity and just prolongs the required measurement time, with our dilute nuclei of supported materials often we could not obtain any ³¹P NMR signal at all any longer, no matter how

long the measurement time was allowed to be. Successful suspension NMR of these samples, however, convinced us that the catalyst was still there and intact, and that it was not some metallic or paramagnetic particles or absence of metal complex that prevented the successful measurement and/or efficient CP.

For problems that arise from the splitting of the HH match at higher MAS frequencies, some approaches have already been described. Since these main strategies, namely those concerning mechanical methods, special radiofrequency (r.f.) techniques or alternative means of polarization transfer, such as dynamic nuclear polarization, have been well reviewed by Michel and Engelke,³² here we give only selected and more recent references. Of all the possible solutions, only the r.f. techniques are applicable to our materials: dynamic nuclear polarization would, for example, require free or unpaired electrons. Mechanical methods, such as spinning at other than the magic angle,³² for example at 90°, are not practical at a spectrometer in a 'central' NMR facility, where a large number of routine samples have to be measured. Even most special pulse sequences,^{43–48} among them the popular ones applying a ramp in the S (dilute nuclei) or I (abundant nuclei) channels,^{35,49–55} often require rotor synchronization or at least special skill in adjusting the pulse durations and power levels. Furthermore, most of the presented techniques used ¹³C NMR of isotopically enriched samples, and rather 'easy' compounds.

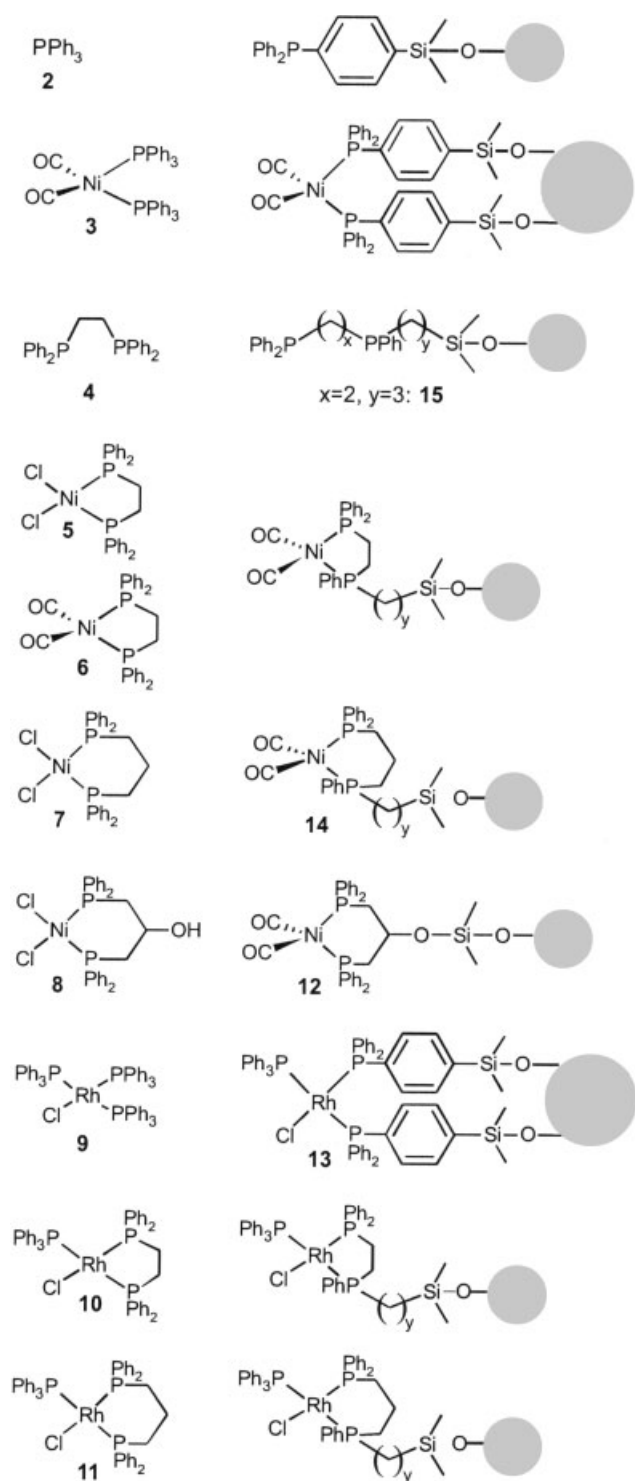
Therefore, we started to investigate the ³¹P CP characteristics of our ligands, metal complexes and immobilized catalysts in more detail. Our goal was to find an easy, uncomplicated and general strategy for the fast, routine measurements of difficult samples with low contents of ³¹P nuclei using high rotational frequency MAS and reasonably efficient CP. Our alternative approach makes use of model compounds that mimic the proton surroundings of the ³¹P nuclei, and in this way display the ¹H-³¹P HH characteristics of suitable 'real-life' samples. This new strategy, together with systematic and detailed studies of measurement parameters such as contact times and filling factors, is presented here and compared with a ramp method applied previously.

RESULTS AND DISCUSSION

Model compounds for immobilized phosphines and catalysts

Nearly all of the transition metal complexes used as homogeneous or immobilized catalysts contain phosphine ligands. The latter most often feature tertiary phosphines, because these are more robust, easy to synthesize and handle and often air-stable. The tertiary phosphines can again be divided into the categories of triarylphosphines and alkyl diarylphosphines. Phosphines with more than one alkyl substituent are rarely encountered, because these are less stable towards oxidation and more basic, and hence not as favorable for catalysis. This overall scenario fortunately has the consequence that in an NMR spectroscopic sense, there is not much change in the surroundings of the ³¹P nucleus. Therefore, it should be possible to determine a handful of commercially available or easy to synthesize

model compounds, optimize their measurement parameters and apply these to a wide variety of 'real-life' phosphines, their metal complexes and immobilized catalysts. The NMR spectroscopic behavior of the ^{31}P nuclei should not differ substantially when the species are immobilized, as our previous work shows. We applied model compounds such as those shown in Scheme 2 for our studies of 'real-life' samples.



Scheme 2. Model compounds and examples of their analogs immobilized on silica.^{8,10,19} $x, y = 2, 3$.

Hartmann-Hahn matching profiles of model compounds and a new strategy for measuring 'real-life' samples

It is predominantly the homonuclear dipolar ^1H - ^1H interactions which lead to a splitting of the HH matching profiles into a centerband and sidebands when the MAS frequency reaches comparable values.³² However, during the CP process, I-I and I-S spin correlations are not independent of each other, and several cases have been described³² that indicate that heteronuclear dipolar interactions are also important. For example, quaternary carbons always display more pronounced splitting in their matching profiles than CH_n groups in the same system.^{32,46} The influence of the heteronuclear dipolar interactions on the splitting of the matching profiles is also visible in ^{19}F - ^{29}Si CP.^{43,45}

All of our phosphines are tertiary, which is on the one hand convenient, because the measurements can be done with compressed air instead of nitrogen. However, it also means that there are no ^1H nuclei bound directly to ^{31}P , and therefore the heteronuclear dipolar interactions are weaker than in secondary phosphines. Hence the HH matching profiles of the studied compounds split into a centerband and sidebands already at low MAS speeds (see below). In an NMR sense, the model compounds can be divided further into two categories: substances with alkyl substituents at phosphorus, and those with triarylphosphines. Even these two categories of the above model compounds already show differences in the matching profiles. As exemplified in Fig. 1 for $\text{Cl}_2\text{Ni}(\text{dppf})$ (5) and $(\text{CO})_2\text{Ni}(\text{PPh}_3)_2$ (3), the matching profile of the latter is split into separate bands already at a 4 kHz rotational speed, whereas the profile of the alkyldiarylphosphine compound still looks smooth. Whether this is attributable to the fact that the heteronuclear dipolar ^1H - ^{31}P interactions are much weaker for 3 than for 5, which contains many alkyl protons in the vicinity of phosphorus, or whether this is entirely due to different homonuclear dipolar ^1H - ^1H interactions, will be the subject of further investigation.

At higher MAS speeds, the matching profiles of all the model compounds split into the characteristic bands, as exemplified for $\text{Cl}_2\text{Ni}(\text{dppp})$ (7) in Fig. 2. The bands have

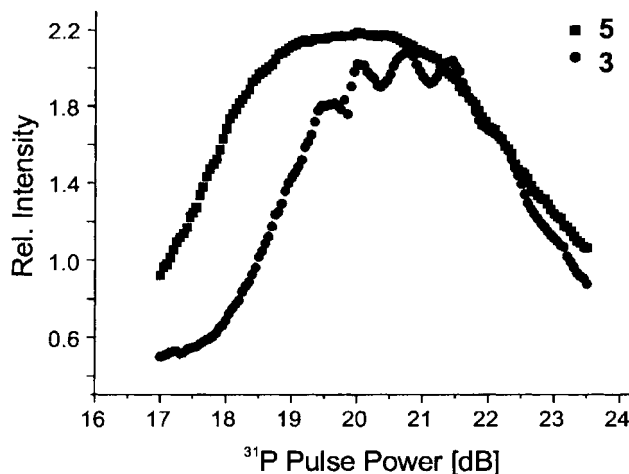


Figure 1. HH matching profiles of $(\text{CO})_2\text{Ni}(\text{PPh}_3)_2$ (3) and $\text{Cl}_2\text{Ni}(\text{dppf})$ (5) at 4 kHz rotational frequency.

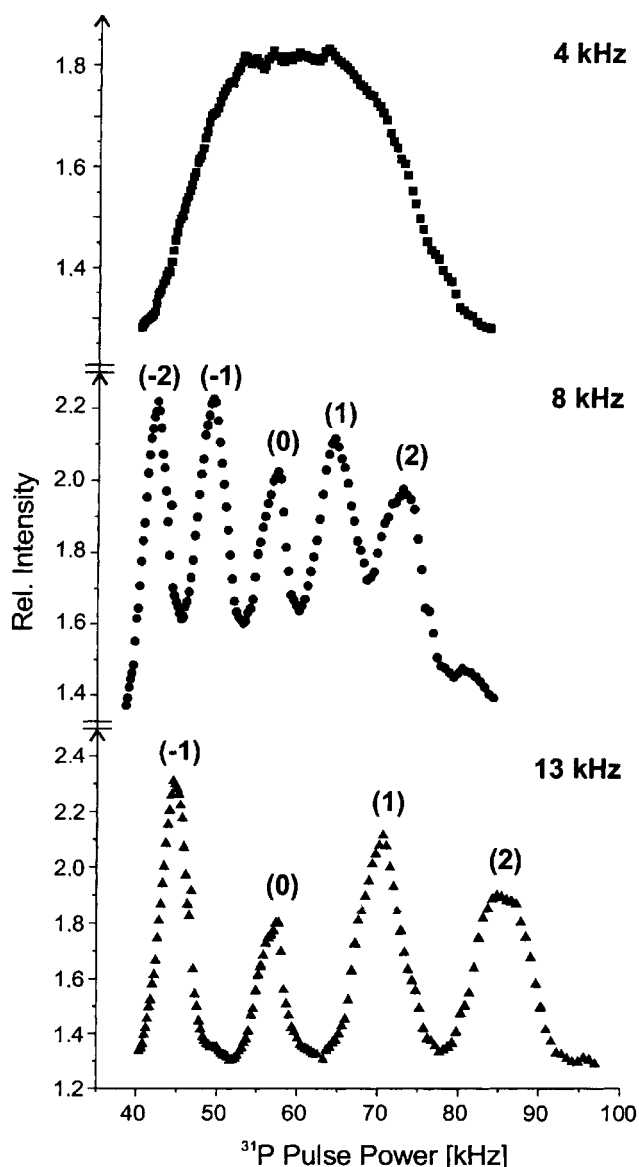


Figure 2. HH matching profiles of $\text{Cl}_2\text{Ni}(\text{dppp})$ (7) at MAS frequencies of 4, 8 and 13 kHz.

approximately the distance of the rotational frequencies between one another. In addition to the center band, which corresponds to the ^1H and ^{31}P values of the exact HH match, there are bands of first and second order, which we denoted according to the convention (e.g. Ref. 35) in Fig. 2.

As outlined recently,³³ the matching profiles can be derived either from the signal intensities of the FIDs or from the integrals of the signals in the spectra. The latter give higher and more precise values because the rotational sidebands of the signals are included. However, for determining the integral the FID has to be transformed. Making use of signal intensities from the FID directly is more practicable, and in our cases does not make a qualitative difference, as we found after checking carefully. Therefore, we basically used FID signal intensities, and only occasionally signal integrals, for recording the matching profiles.

The center band is mostly supported by magnetization, which is transferred via scalar $J(^{31}\text{P}, ^1\text{H})$ couplings, as outlined

for example in Ref. 36. Since the $^{2/3}J$ couplings to neighboring protons are rather small in our model compounds,^{9,17,19} the intensity of the center band of the matching profiles can also be expected to be reduced. Indeed, this can be seen, e.g., for the nickel compound 7 in Fig. 2. The matching profiles of the model compounds are all different from the one of $\text{NH}_4\text{H}_2\text{PO}_4$ (1). This is the main reason why $\text{NH}_4\text{H}_2\text{PO}_4$ no longer works as an HH standard sample for our applications at higher rotational speeds. The bite angles of the chelating phosphines are seemingly irrelevant, the HH matching profiles of dppe- and dppp-type compounds being practically identical. However, the nature of the metal matters. So, for example, the profiles of the nickel complexes 5–8 resemble each other, but they differ from the profiles of 10 and 11. Taking this into account, our new strategy makes use of the matching profiles of the model compounds: the measurement parameters of the highest maximum are chosen, which is most often the first order sideband with less ^{31}P power [(-1), see Fig. 2], and applied to a 'real-life' sample of the same category with similar proton surroundings of phosphorus. Since all new NMR instruments are digital, the pulse powers are stable over weeks and months. Hence the once determined optimal parameters just have to be read in prior to a measurement.

Dependence of the HH matching profiles on contact time

In the literature, major changes of the HH matching profiles with increasing contact time are reported (e.g. Ref. 42). Therefore, we investigated whether this would also be the case for our model compounds. Fortunately, the positions of the bands in the HH matching profiles do not change when the contact time is increased from 1 to 5 ms, our longest contact time for 'real-life' samples. They are, however, somewhat broadened, and additional bands and shoulders are emerging, as the example of $\text{NH}_4\text{H}_2\text{PO}_4$ (1) in Fig. 3 shows.

Regarding the favorable broadening of the matching profiles, one might in principle think that it would always be best to choose longer contact times. However, the following section explains that the efficiency of the magnetization

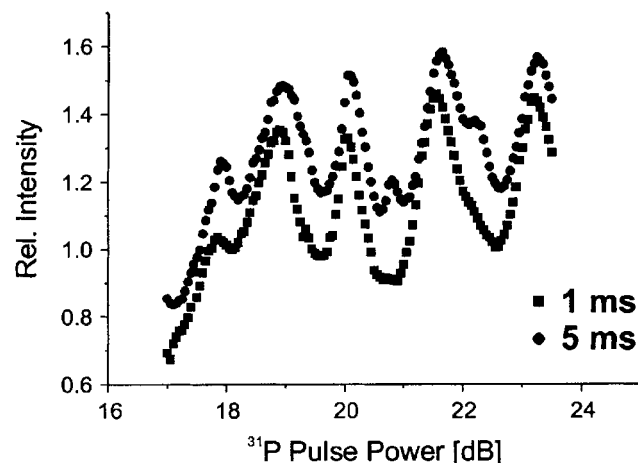


Figure 3. HH matching profile of $\text{NH}_4\text{H}_2\text{PO}_4$ (1) at 8 kHz rotational speed, with contact times of 1 and 5 ms.

transfer also has to be taken into account, which is different for every category of substance.

Dependence of magnetization transfer on contact time

Although, as outlined above, the HH matching profiles are nearly independent of the contact times used, nevertheless, to obtain optimum signal intensities, at least some knowledge about the best contact times for different sample categories is necessary. As a rough estimate based on the time constant T_{HP} ,³² the stronger the heteronuclear dipolar interactions are in a sample, the faster the magnetization transfer and the shorter the contact pulse can be. The heteronuclear dipolar interactions should increase with the number of alkyl protons present in the vicinity of phosphorus. Indeed, for phosphines with at least one alkyl substituent, and their metal complexes, the ^{31}P signal integrals, which include all rotational sidebands, are most intense at short contact times (Fig. 4). On the other hand, weakly coupled spins should require longer contact times in order to allow for magnetization transfer.⁵³ Therefore, if the protons are further away from the ^{31}P nucleus, as in $\text{NH}_4\text{H}_2\text{PO}_4$ (1), or in triarylphosphines such as PPh_3 (2) or their complexes, longer contact times should be favorable. Indeed, this behavior is observed for most of our compounds (Fig. 5). However, this reasoning is somewhat oversimplified, because the plots for contact time dependence, such as those shown for our model compounds in Figs 4 and 5, are not only dependent on T_{HP} and $T_{1\rho}(^1\text{H})$, described theoretically,⁵⁶ and applied, for example, by Jeschke and Grossmann.³⁷ Since in our molecules there are always at least two phosphorus nuclei in close proximity, and ^{31}P is isotopically abundant (100%), $T_{1\rho}(^{31}\text{P})$ has to be considered in addition. The influence of the latter might be responsible, for example, for the irregular behavior of the curve for Wilkinson's catalyst (9) (Fig. 5). This will be the subject of further studies. In the related case of fluorinated polymers, the cross-polarization dynamics between ^1H and ^{19}F have recently been analyzed in detail by Harris and co-workers.^{57,58}

In order to check whether this trend might be changed or even reversed at different spinning speeds, we tested all

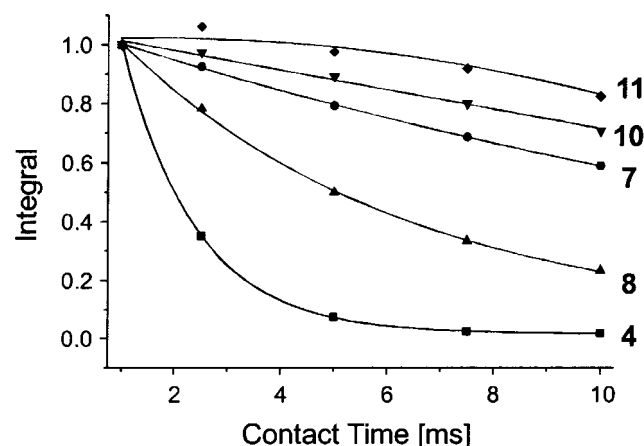


Figure 4. Correlation of the signal integrals of compounds 4, 7, 8, 10 and 11 with contact times of 1–10 ms at 4 kHz rotational frequency.

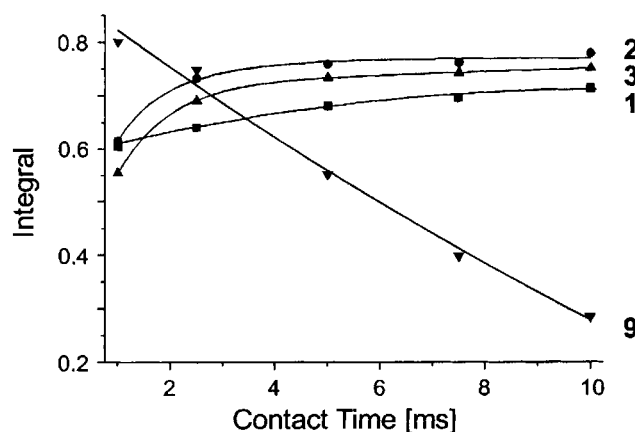


Figure 5. Dependence of the signal intensities of compounds 1, 2, 3 and 9 on the contact times at 8 kHz rotational frequency.

samples at 4, 8 and 13 kHz using the above range of contact times. Despite some minor deviations, the tendencies stayed the same in every case, as shown for, e.g., $\text{Cl}_2\text{Ni}(\text{dppe})$ (5) in Fig. 6.

The half-widths of the signals do not follow a general trend, although in most cases they are diminished by up to 10 Hz on going from a contact time of 1 to 10 ms. Increasing the spinning speed from 4 to 13 kHz under the same conditions often increases the signal half-widths by up to 20 Hz. Since the ^{31}P chemical shifts change somewhat with temperature, this line broadening might be due to an increased temperature gradient along the rotor with faster sample spinning.¹³ However, taking into account that the half-widths of the ^{31}P signals of our model compounds are in the range of several hundred hertz (maximum for 8, 350 Hz), these changes are not very spectacular.

To sum up this section, independent of the spinning speed and the matching profiles, phosphines with at least one alkyl substituent and their metal complexes are best measured with a contact time of ~ 1 ms. Triarylphosphines and their nickel complexes need contact times of at least 5 ms.

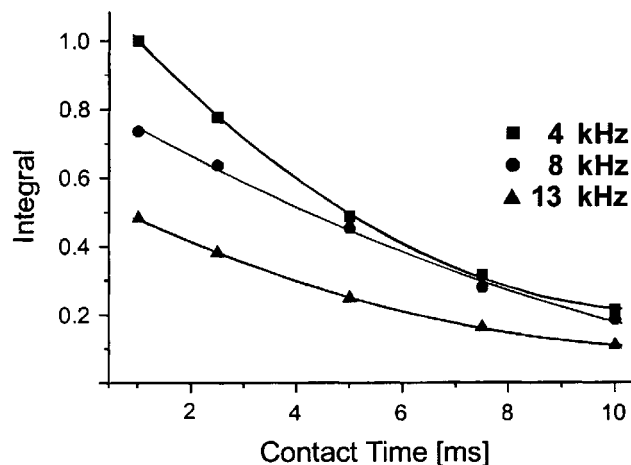


Figure 6. Dependence of the signal integrals of $\text{Cl}_2\text{Ni}(\text{dppe})$ (5) on the contact time at different MAS rates.

Dependence of the HH matching profiles on the ^1H pulse powers

In principle, the HH match can be obtained by varying the ^{31}P or alternatively the ^1H pulse power, while leaving the other one constant. However, the conventional way nowadays is to keep the proton pulse power fixed after determination of the 90° pulse, and then the ^{31}P irradiation power is varied until the HH match is reached. Since one starts with the choice of the proton pulse power, for our application it is crucial to know its influence on the resulting HH matching profile. We studied most of the model compounds applying different ^1H pulse powers, and found that an increase in proton pulse power generally results in enhanced signal intensities, and more pronounced maxima in the HH matching profiles. In a typical case, e.g. $\text{Cl}_2\text{Ni}(\text{dppp})$ (7), an increase in the ^1H pulse power from 12.19 to 10.72 dB (corresponding to 90° pulse durations of 5.4 and 4.2 μs) leads to a more structured HH matching profile with more pronounced minima and maxima with slightly narrower bands (see Fig. 7). This is probably due to the fact that with lower pulse powers the B_1 inhomogeneity along the rotor is more pronounced than with higher pulse powers that provide a more homogeneous r.f. field. The positions of the bands in the HH matching profile do not change substantially with the proton pulse powers. Hence, a change of pulse powers should not affect our new measurement strategy of using the most intense peak for the HH match. However, the higher the ^1H pulse powers, the better should be the resulting signal-to-noise ratio in the spectrum, as long as one stays within safe boundaries.

Different sample volumes and the effect on their HH matching profiles

For surface-immobilized species, which are very dilute with respect to the support material, it is advantageous to maximize the sample volume and fill the whole rotor in order to increase the achievable signal-to-noise ratio. On the other hand, often the polycrystalline precursors or model compounds are more conveniently packed and measured using laboratory-made air-tight PTFE spacers fixed in the rotor, so that the substance is only filled up to 4 mm high in the center part of the rotor. As has been well described,^{35,53} the B_1 field strength is about twice as high in the middle of a

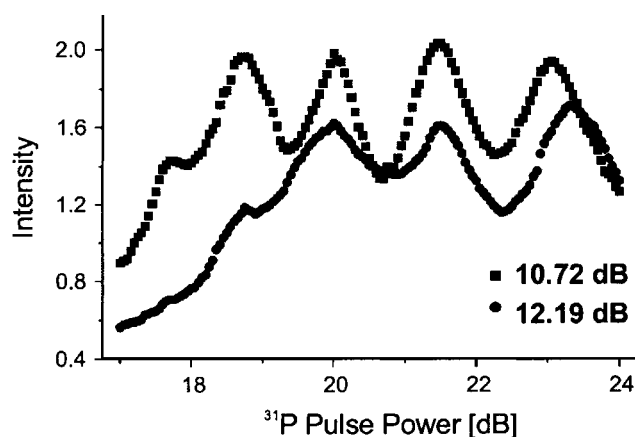


Figure 7. HH matching profiles of $\text{Cl}_2\text{Ni}(\text{dppp})$ (7) at ^1H pulse powers of 10.72 and 12.19 dB at 8 kHz rotational frequency.

rotor than at the top or bottom. For the center band of the HH matching profile, where only the $B_1(^1\text{H})/B_1(^{31}\text{P})$ ratio counts, this does not make any difference, because the ^1H and ^{31}P fields change equally, and so the ratio stays the same and the HH match remains intact. However, at the sidebands of the matching profile, the deviations $\Delta\omega$ from the match change, owing to the different frequencies of the ^1H and ^{31}P nuclei. Since our strategy usually makes use of the most intense first sideband, the conditions could be very different for full rotors as compared with those with PTFE spacers. Therefore, in order to check whether the measurement parameters derived from our model compounds with small sample volumes could still be applied to the samples with full rotors, we studied the HH matching profiles of some model compounds at different spinning speeds. Fortunately, compounds with triarylphosphine ligands behave in the same way as those with diarylalkylphosphines. Figure 8 shows the matching profiles of $(\text{CO})_2\text{Ni}(\text{PPh}_3)_2$ (3) as a representative example.

At 13 kHz spinning speed, we observe the behavior already reported by Metz *et al.*³⁵ The matching bands are, of course, less intense, but also narrower for the centered sample with reduced volume, as compared with that in the full rotor. In the latter case especially the negative sidebands show a broad shoulder, because lower $B_1(^{31}\text{P})$ fields are needed to compensate for the reduced field strengths. Interestingly, however, the splitting of the HH matching profiles always starts at lower spinning speeds than in the case of samples with PTFE spacers as displayed in Fig. 8 at 4 kHz. While

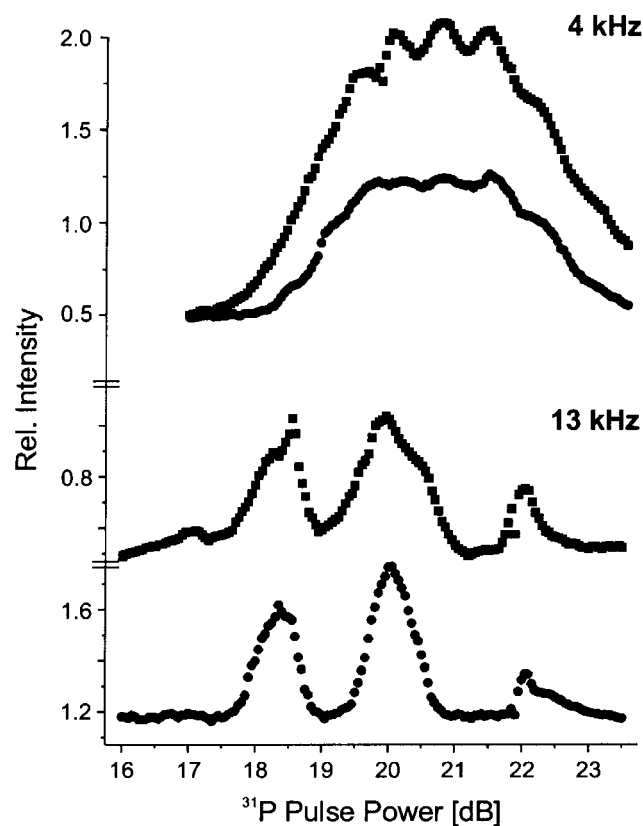


Figure 8. Comparison of the HH matching profiles of $(\text{CO})_2\text{Ni}(\text{PPh}_3)_2$ (3) at MAS rates of 4 and 13 kHz. (■) Fully packed rotor; (●) substance in rotors with PTFE spacers (see text).

we are still trying to find the proper explanation for this phenomenon, for the moment we assume that it might be the lower overall intensity that makes the HH matching profiles from the smaller sample sizes look smoother.

However, what is most important for our new strategy is that the positions of the maxima in the HH matching profiles do not change substantially with the sample volumes. Therefore, the measurement parameters obtained from small volumes of model compounds can be applied to rotors full of supported material and vice versa.

Comparison of CP and ramp spectra

Pulse sequences using a ramp^{35,49–55} are very useful and popular, as they usually also substantially reduce the residual linewidths of the signals in the spectra. A comparison of the ³¹P spectra of polycrystalline Wilkinson's catalyst **9** as measured with a ramp sequence and conventional CP shows the clear advantage of a ramp (Fig. 9): the ¹J(¹⁰³Rh,³¹P) and ²J(³¹P,³¹P) couplings⁸ are much better resolved. As already discussed, for example, by Bowmaker *et al.*³⁴ and Jeschke and Grossmann,³⁷ the intensities of the rotational sidebands also change with the CP sequence used. For precise determinations of CSAs, this would of course be a major problem. However, for our applications the isotropic chemical shifts are most important, since the CSA is reduced substantially anyway, on going from the polycrystalline to the corresponding immobilized species, as demonstrated, for example, for **13** in Ref. 8.

Therefore, at this point, it makes sense to test whether a ramp method could compete with our new strategy, especially with respect to the achievable signal half-widths and intensities.

Ramp pulse sequences for ³¹P are most favorable for rotors with large sample sizes, because the bands in the HH matching profile are broader at higher spinning speeds (see above), and therefore more signal intensity can be obtained using a ramp going ideally over the whole first-order sideband. In the matching profiles of the model compounds

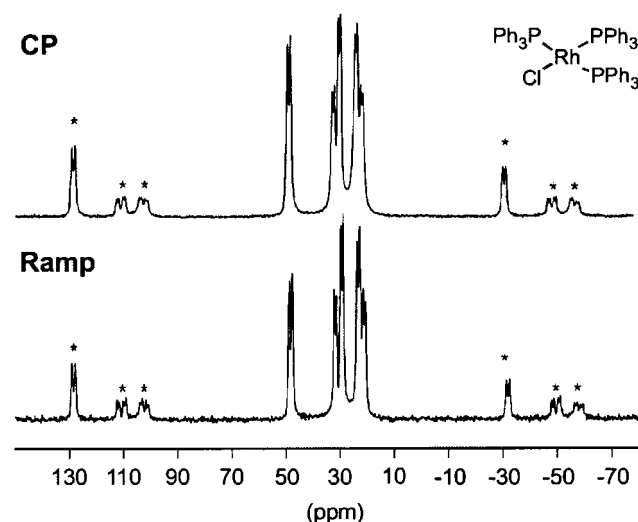


Figure 9. ³¹P spectra of ClRh(PPh₃)₃ (**9**) recorded at a MAS frequency of 13 kHz with conventional CP/MAS, and with a ramp pulse sequence.

the bands have a width of about 3 dB. Therefore, in order to check all possibilities at 8 and 13 kHz rotational speed, we first established the HH match with NH₄H₂PO₄ as the standard and subsequently used the ramp sequence for measuring (method **a**). Then, regarding the HH matching profiles of the model compounds, we applied three different starting points for a ramp decreasing linearly in 64 steps in the proton channel. In method **b** we chose the deepest valley next to an intense band at the low-frequency side, for measurement **c** the most intense maximum, which was often the (−1) band, and for **d** the second highest band (often +1) (Fig. 2). For comparison, we measured the spectra of the same compounds with conventional CP, using the parameters obtained again from the corresponding matching profiles: Measurements **e–h** were conventional CP sequences using NH₄H₂PO₄ as a HH standard (**e**), using the parameters from the deepest valley (**f**), the highest maximum (**g**) and the second highest maximum (**h**). The results concerning the signal intensities and half-widths are displayed graphically for a representative case, (CO)₂Ni(PPh₃)₂ (**3**), in Figs 10 and 11.

The data for all the other model compounds are given in Tables 1 and 2. The ramp sequence especially showed its merit regarding the half-widths of the signals at medium spinning speed (Fig. 11). The starting point does not matter much in this case. However, the CP sequences give comparable half-widths at higher MAS frequencies. Furthermore, the signal intensities are highest for method **g** at all rotational speeds and for all compounds. Therefore, we conclude that the best method to measure phosphines and their metal complexes is recording the HH matching profile, which requires about 45 min, and then choosing the parameters of the highest maximum for the CP measurement. For example, the ³¹P CP/MAS spectrum of compound **8** in Fig. 12 was recorded within 30 min. There are two phosphorus resonances, because both ³¹P nuclei are magnetically inequivalent in the solid state.

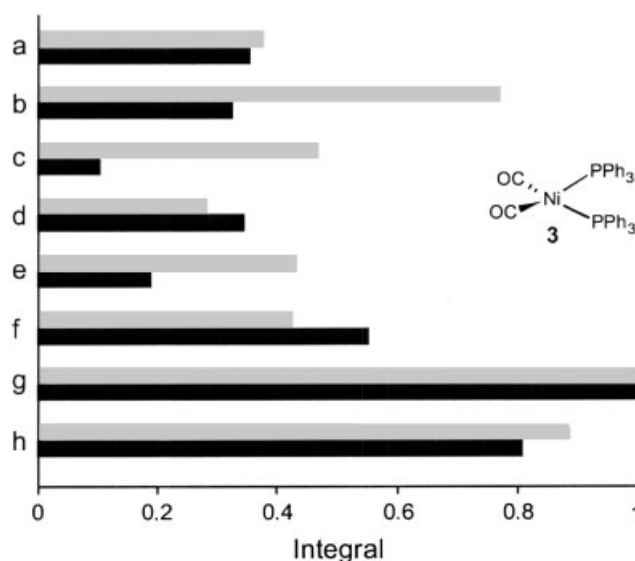


Figure 10. Signal intensities of (CO)₂Ni(PPh₃)₂ (**3**) obtained after recording the ³¹P spectra with methods **a–h** (see text) at MAS frequencies of 8 (gray) and 13 (black) kHz.

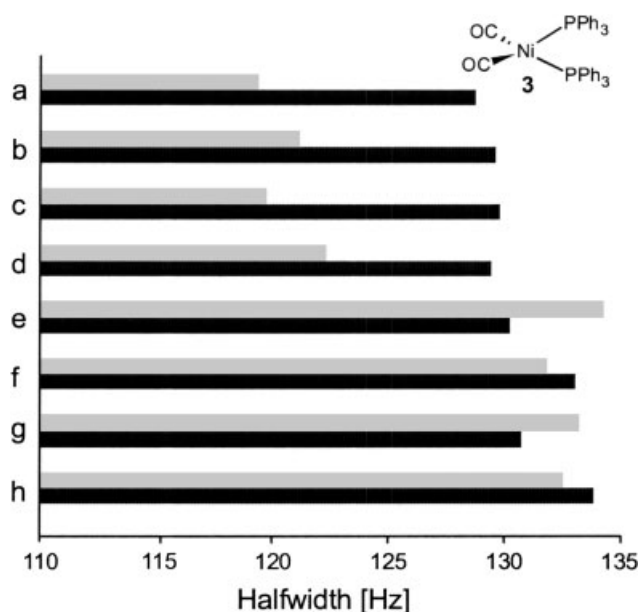


Figure 11. Half-widths of the signals of $(\text{CO})_2\text{Ni}(\text{PPh}_3)_2$ (**3**) obtained after recording the ^{31}P spectra with methods **a–h** (see text) at MAS frequencies of 8 (gray) and 13 (black) kHz.

Since 'real-life' samples, such as immobilized species, do not allow the recording of their HH matching profile, and therefore one cannot determine the position of the most intense sideband exactly, one has to choose the best fitting model compound, and just apply the parameters found there. The examples below show that this approach works very well, and spectra with good signal-to-noise ratios can be obtained within reasonable measurement times.

Some applications of the new strategy to immobilized species

In comparison with conventional CP and the ramp method, the signal-to-noise ratio of all signals, not only the phosphine

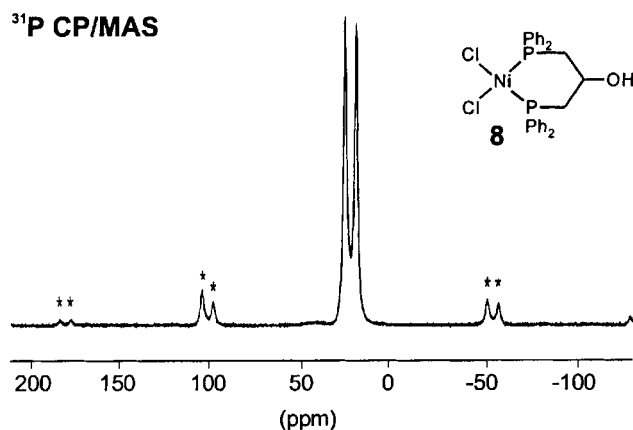


Figure 12. ^{31}P CP/MAS spectrum (method **g**) of polycrystalline **8** in a rotor with PTFE spacers after a 30 min measurement time at a rotational frequency of 13 kHz.

resonance but also the signal of the oxidic species, improves with our new strategy, as displayed in Fig. 13.

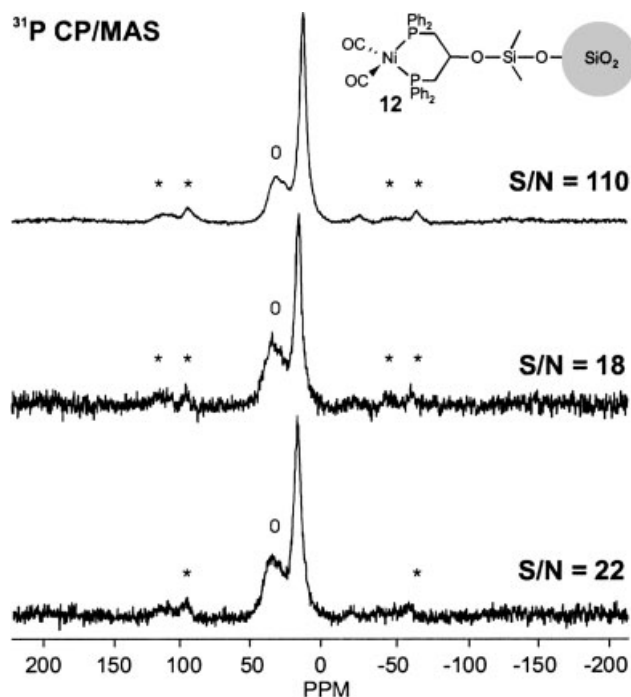
This shows that although we would never try to evaluate CP/MAS spectra quantitatively without detailed studies such as variations of contact times, at least with our method we are not any worse off than with conventional CP and ramp methods with respect to integration. However, the signal-to-noise ratio of 110 that we obtain with our strategy is much better than that from other methods (18 and 22, see Fig. 13). We have already demonstrated the wide-ranging applicability of our approach by successfully recording the spectra of a plethora of metal complexes from other groups in our department, both polycrystalline and immobilized on different types of supports. With the improvement regarding measurement times, we can now also afford to run a large number of routine samples. For example, we could determine that chelating phosphines such as **15** are much more stable towards oxidation after they have been immobilized on silica. While they are oxidized quickly in solution as soon as oxygen is admitted, it takes 4 days of air exposure of the

Table 1. ^{31}P signal intensities of the model compounds **1–11** at 8/13 kHz rotational speed, after measurement with methods **a–h** (see text for details): **(a)** ramp measurement with **1** as HH standard; **(b)** ramp starting at deepest HH valley; **(c)** ramp starting at highest HH maximum; **(d)** ramp starting at second highest maximum; **(e)** CP with parameters derived from **1**; **(f)** CP with parameters from deepest HH valley; **(g)** CP with parameters from highest maximum; **(h)** CP with parameters from second highest maximum

No.	Compound	Integrals obtained by methods a–h							
		a	b	c	d	e	f	g	h
1	$\text{NH}_4\text{H}_2\text{PO}_4$	0.68/0.68	0.49/0.64	0.64/0.16	0.85/0.2	0.62/0.23	0.53/0.22	1.00/1.00	0.96/0.75
2	PPh_3	0.57/0.67	0.37/1.03	0.46/0.26	0.75/0.78	0.43/0.26	0.38/0.31	1.00/1.00	0.97/0.90
3	$(\text{CO})_2\text{Ni}(\text{PPh}_3)_2$	0.35/0.38	0.32/0.77	0.10/0.46	0.34/0.28	0.19/0.43	0.55/0.42	1.00/1.00	0.80/0.89
4	dppe	0.62/0.80	0.62/0.36	0.59/0.52	0.62/0.65	0.75/0.60	0.64/0.49	1.00/1.00	0.96/0.99
5	$\text{Cl}_2\text{Ni}(\text{dppe})$	0.67/0.62	0.76/0.71	0.77/0.24	0.26/0.30	0.77/0.50	0.71/0.44	1.00/1.00	1.00/0.95
6	$(\text{CO})_2\text{Ni}(\text{dppe})$	0.53/0.50	0.77/0.78	0.76/0.27	0.27/0.27	0.81/0.48	0.49/0.69	1.00/1.00	0.99/0.94
7	$\text{Cl}_2\text{Ni}(\text{dppp})$	0.82/0.65	0.81/0.78	0.61/0.27	0.78/0.27	0.87/0.52	0.79/0.37	1.00/1.00	0.99/0.90
8	$\text{Cl}_2\text{Ni}(\text{PPh}_2\text{CH}_2)_2\text{CHOH}$	0.73/0.67	0.80/0.54	0.78/0.19	0.53/0.20	0.61/0.32	0.57/0.29	1.00/1.00	1.00/0.72
9	$\text{ClRh}(\text{PPh}_3)_3$	0.75/0.42	0.50/0.36	0.97/0.19	0.20/0.61	0.53/0.31	0.47/0.23	1.00/1.00	0.94/0.91
10	$\text{Cl}(\text{PPh}_3)_2\text{Rh}(\text{dppe})$	0.59/0.35	0.70/0.21	0.65/0.73	0.72/0.13	0.59/0.46	0.74/0.17	1.00/1.00	0.99/0.80
11	$\text{Cl}(\text{PPh}_3)_2\text{Rh}(\text{dppp})$	0.62/0.32	0.86/0.21	0.82/0.74	0.86/0.20	0.70/0.55	0.79/0.19	1.00/1.00	0.98/0.75

Table 2. Half-widths of the ^{31}P signals of the model compounds **1–11** at 8/13 kHz rotational speed, after measurement with methods **a–h** (see text for details and Table 1).

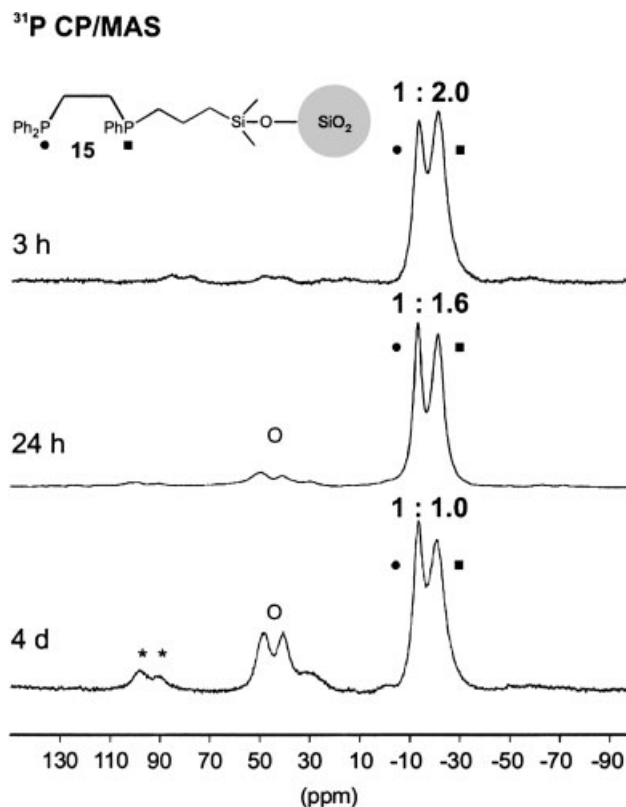
No.	Compound	Half-widths (Hz) obtained by methods a–h							
		a	b	c	d	e	f	g	h
1	$\text{NH}_4\text{H}_2\text{PO}_4$	28/34	43/58	24/35	33/60	160/279	187/372	152/342	152/419
2	PPh_3	52/56	52/65	51/78	51/60	59/60	60/71	61/82	58/70
3	$(\text{CO})_2\text{Ni}(\text{PPh}_3)_2$	93/119	98/121	98/120	97/122	101/134	115/132	103/133	118/132
4	dppe	110/131	112/161	107/154	108/152	122/155	122/164	119/147	119/145
5	$\text{Cl}_2\text{Ni}(\text{dppe})$	189/195	192/200	190/204	194/204	197/204	202/219	202/205	203/220
6	$(\text{CO})_2\text{Ni}(\text{dppe})$	107/108	109/108	105/110	109/114	120/119	120/125	119/118	120/130
7	$\text{Cl}_2\text{Ni}(\text{dppp})$	269/279	274/281	270/283	270/294	278/285	278/297	284/294	282/312
8	$\text{Cl}_2\text{Ni}(\text{PPh}_2\text{CH}_2)_2\text{CHOH}$	332/335	330/339	326/368	335/347	366/377	370/405	364/373	369/407
9	$\text{ClRh}(\text{PPh}_3)_3$	265/268	278/277	268/178	272/275	282/286	296/196	289/288	289/327
10	$\text{Cl}(\text{PPh}_3)\text{Rh}(\text{dppe})$	278/283	279/305	277/309	279/336	290/294	289/347	235/346	325/356
11	$\text{Cl}(\text{PPh}_3)\text{Rh}(\text{dppp})$	657/687	636/661	637/668	640/653	669/703	649/681	646/667	645/662

**Figure 13.** ^{31}P spectra of **12**, recorded with methods **g** (upper trace), **c** (middle) and **e** (bottom) (see text), with 13 kHz rotational speed. Circles denote oxidic byproducts.

silica systems on the bench until the immobilized phosphines show substantial traces of oxides in the spectra (Fig. 14). As expected, the dialkylarylphosphine moiety is more air-sensitive.

CONCLUSION

We have developed a new strategy for ^{31}P CP/MAS measurements of polycrystalline and immobilized phosphines and metal complexes at high rotational speeds. We have demonstrated that the best method to deal with difficult, dilute samples at high MAS frequencies is first to record the matching profiles of corresponding model compounds.

**Figure 14.** ^{31}P spectra of **15** recorded with the new strategy **g** (see text) at 8 kHz rotational speed after the indicated times of air exposure. Circles denote the oxide signals. The ratios of the integrals were obtained after deconvolution.

These can be used for determining the optimum CP parameters, which are then successfully applied to measurements of the corresponding 'real-life' substances or materials. We have compared conventional ramp and CP methods with the new strategy. The latter gives on the whole more intense signals and higher signal-to-noise ratios. The new strategy is important, because it provides a basis for quick, routine solid-state NMR measurements of immobilized species, that are rapidly gaining importance in many fields of chemistry.

EXPERIMENTAL

All the spectra were recorded on a digital Bruker Avance 400 NMR spectrometer equipped with an ultrashield wide-bore magnet and a 4 mm multinuclear double-bearing MAS probehead. The polycrystalline molecular compounds were densely packed, modified silicas filled loosely into the ZrO₂ rotors in a glove-box. For the rhodium species, laboratory-made PTFE spacers were fixed at the top and bottom of the rotors, so that only about 4 mm of the middle part of the rotors was filled with sample material. CP and MAS with rotational speeds between 4 and 15 kHz were applied, as described in the text. The ³¹P CP/MAS NMR spectra were referenced with respect to 85% aqueous H₃PO₄ by setting the ³¹P NMR peak of solid NH₄H₂PO₄ to +0.81 ppm. The HH matches and contact times were set as described in the text. For the exponential multiplication a line-broadening factor of 20–50 Hz was applied for spectra of immobilized species. The recycle delay was 10 s for all samples. Typical numbers of transients were 16 for polycrystalline phosphines and 128 and 512 for molecular nickel and rhodium compounds, respectively. Immobilized catalysts needed measurement times of 3–6 h, with about 2000 as a typical number of transients.

The molecular and surface-bound complexes and phosphines were synthesized as described previously.^{8,9,17,19}

Acknowledgments

We thank the Deutsche Forschungsgemeinschaft (DFG) for support via the Landesforschungsschwerpunkt "Katalyse", and the Fonds der Chemischen Industrie (FCI) for financial support. We thank Dr H. Förster (Bruker) for helpful discussions and the Bruker company for a very generous gift of an accessory for our new Avance 400 NMR instrument. We are also grateful for the help of Mrs D. Rambow, who prepared countless samples and packed them into rotors.

REFERENCES

- (a) Nicolaou KC, Hanks R, Hartwig W (eds). *Handbook of Combinatorial Chemistry*, vols 1 and 2. Wiley-VCH: Weinheim, 2002; (b) Wilson SR, Czarnik AW (eds). *Combinatorial Chemistry*. Wiley: New York, 1997; (c) Bannworth W, Felder E (eds). *Combinatorial Chemistry*. Wiley-VCH: Weinheim, 2000; (d) Jung G. *Combinatorial Chemistry*. Wiley-VCH: Weinheim, 1999.
- (a) Seneci P. *Solid-phase Synthesis and Combinatorial Technologies*. Wiley: New York, 2000; (b) Zaragoza Dörwald F. *Organic Synthesis on Solid Phase*. Wiley-VCH: Weinheim, 2000.
- Vansant EF; VanDer Voort P, Vrancken KC. *Characterization and Chemical Modification of the Silica Surface*. Elsevier: Amsterdam, 1995.
- (a) Scott RPW. *Silica Gel and Bonded Phases*. Wiley: New York, 1993; (b) Subramanian G. *A Practical Approach to Chiral Separations by Liquid Chromatography*. VCH: Weinheim, 1994.
- Hartley FR. *Supported Metal Complexes*. Reidel: Dordrecht, 1985.
- Clark JH, Kybett AP, Macquarrie DJ. *Supported Reagents*. Verlag Chemie: Weinheim, 1992.
- (a) DeVos DE, Vankelecom IFJ, Jacobs PA (eds). *Chiral Catalyst Immobilization and Recycling*. Wiley-VCH: Weinheim, 2000; (b) Clark JH. *Catalysis of Organic Reactions by Supported Inorganic Reagents*. VCH: Weinheim, 1994.
- Merckle C, Haubrich S, Blümel J. *J. Organomet. Chem.* 2001; **627**: 44.
- Behringer KD, Blümel J. *Inorg. Chem.* 1996; **35**: 1814.
- Reinhard S, Soba P, Rominger F, Blümel J. *Adv. Synth. Catal.* 2003; **345**: in press.
- Reinhard S, Behringer KD, Blümel J. *New J. Chem.* 2003, in press.
- Merckle C, Blümel J. *Adv. Synth. Catal.* 2003; **345**: in press.
- Schnellbach M, Köhler FH, Blümel J. *J. Organomet. Chem.* 1996; **520**: 227, and references cited therein.
- Blümel J. *J. Am. Chem. Soc.* 1995; **117**: 2112.
- Behringer KD, Blümel J. *J. Liq. Chromatogr.* 1996; **19**: 2753.
- Behringer KD, Blümel J. *J. Chem. Soc., Chem. Commun.* 1996; 653.
- Blümel J. *Inorg. Chem.* 1994; **33**: 5050.
- Merckle C, Blümel J. *Chem. Mater.* 2001; **13**: 3617.
- Tsiavalariis G, Haubrich S, Merckle C, Blümel J. *Synlett* 2001; 391.
- Behringer KD, Blümel J. *Z. Naturforsch., Teil B* 1995; **50**: 1723.
- De Rege FM, Morita DK, Ott KC, Tumas W, Broene RD. *Chem. Commun.* 2000; 1797.
- Duncan TM. *A Compilation of Chemical Shift Anisotropies*. Farragut Press: Chicago, 1990.
- Bell AT, Pines A (eds). *NMR Techniques in Catalysis*. Marcel Dekker: New York, 1994.
- Engelhardt G, Michel D. *High-resolution Solid-state NMR of Silicates and Zeolites*. Wiley: New York, 1987.
- Fyfe CA. *Solid-state NMR for Chemists*. CFC Press: Guelph, ON, 1983.
- Stejskal EO, Memory JD. *High Resolution NMR in the Solid State*. Oxford University Press: New York, 1994.
- Fitzgerald JJ (ed). *Solid-state NMR Spectroscopy of Inorganic Materials*. American Chemical Society: Washington, DC, 1999.
- Schmidt-Rohr K, Spiess HW. *Multidimensional Solid-state NMR and Polymers*. Academic Press: London, 1994.
- Laws DD, Bitter H-ML, Jerschow A. *Angew. Chem., Int. Ed. Engl.* 2002; **41**: 3096.
- Pines A, Gibby MG, Waugh JS. *J. Chem. Phys.* 1973; **56**: 1176.
- Schaefer J, Stejskal EO. *J. Am. Chem. Soc.* 1976; **98**: 1031.
- Michel D, Engelke F. *Cross-polarization, Relaxation Times and Spin-diffusion in Rotating Solids*. *NMR Basic Principles and Progress*, vol. 32. Springer: Heidelberg, 1994; and references cited therein.
- Kolodziejski W, Klinowski J. *Chem. Rev.* 2002; **102**: 613, and references cited therein.
- Bowmaker GA, Harris RK, Oh S-W. *Coord. Chem. Rev.* 1997; **167**: 49, and references cited therein.
- Metz G, Wu X, Smith SO. *J. Magn. Reson. A* 1994; **110**: 219.
- Verhoeven A, Verel R, Meier BH. *Chem. Phys. Lett.* 1997; **266**: 465.
- Jeschke G, Grossmann G. *J. Magn. Reson. A* 1993; **103**: 323.
- Brinkmann A, Levitt MH. *J. Chem. Phys.* 2001; **115**: 357.
- Engelke F, Kind T, Michel D, Pruski M, Gerstein BC. *J. Magn. Reson.* 1991; **95**: 286.
- Zhang S, Wu X, Mehring M. *Chem. Phys. Lett.* 1990; **166**: 92.
- Zhang S, Stejskal EO, Fornes RE, Wu X. *J. Magn. Reson. A* 1993; **104**: 177.
- Meier BH. *Chem. Phys. Lett.* 1992; **188**: 201.
- Fyfe CA, Lewis AR, Chézeau J-M. *Can. J. Chem.* 1999; **77**: 1984.
- Pratima R, Ramanathan KV. *Chem. Phys. Lett.* 1994; **221**: 322.
- Bertani P, Raya J, Reinheimer P, Gougeon R, Delmotte L, Hirschinger J. *Solid State Nucl. Magn. Reson.* 1999; **13**: 219.
- Kolbert AC, Gann SL. *Chem. Phys. Lett.* 1994; **224**: 86.
- Green H, Titman JJ, Spiess HW. *Chem. Phys. Lett.* 1993; **213**: 145.
- Baldus M, Petkova AT, Herzfeld J, Griffin RG. *Mol. Phys.* 1998; **95**: 1197.
- Raya J, Hirschinger J. *J. Magn. Reson.* 1998; **133**: 341.
- Van Rossum B-J, De Groot CP, Ladizhansky V, Vega S, De Groot HJM. *J. Am. Chem. Soc.* 2000; **122**: 3465.
- Fu R, Pelupessy P, Bodenhausen G. *Chem. Phys. Lett.* 1997; **264**: 63.

52. Han M, Peersen OB, Bryson JW, O'Halloran TV, Smith SO. *Inorg. Chem.* 1995; **34**: 1187.
53. Metz G, Ziliox M, Smith SO. *Solid State Nucl. Magn. Reson.* 1996; **7**: 155.
54. Hediger S, Signer P, Tomaselli M, Ernst RR, Meier BH. *J. Magn. Reson.* 1997; **125**: 291.
55. Bennett AE, Rienstra CM, Auger M, Lakshmi KV, Griffin RG. *J. Chem. Phys.* 1995; **103**: 6951.
56. Alemany LB, Grant DM, Pugmire RJ, Alger TD, Zilm KW. *J. Am. Chem. Soc.* 1983; **105**: 2133.
57. Ando S, Harris RK, Monti GA, Reinsberg SA. *Magn. Reson. Chem.* 1999; **37**: 709.
58. Ando S, Harris RK, Reinsberg SA. *J. Magn. Reson.* 1999; **141**: 91.